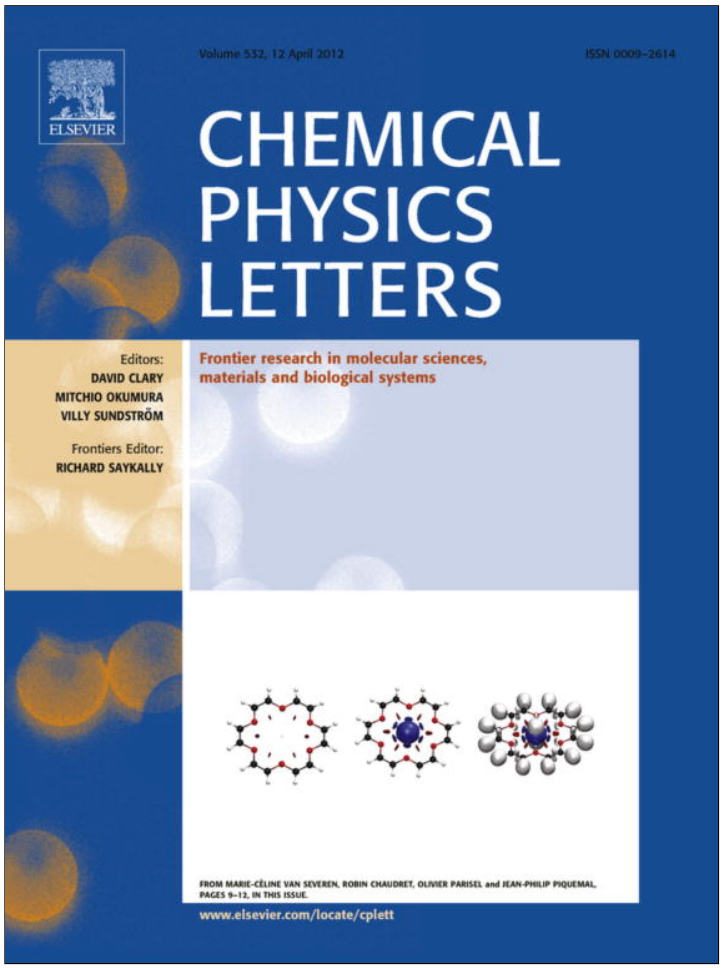

Chemical Physics Letters 532 (2012) 110–115

Contents lists available at SciVerse ScienceDirect

Chemical Physics Letters

journal homepage: www.elsevier.com/locate/cplett

Novel aminobenzanthrone dyes for amyloid fibril detection

Kateryna Vus [a,*], Valeriya Trusova [a], Galyna Gorbenko [a], Elena Kirilova [b], Georgiy Kirilov [b], Inta Kalnina [b], Paavo Kinnunen [c]

[a] Department of Biological and Medical Physics, V.N. Karazin Kharkov National University, 4 Svobody Sq., Kharkov 61077, Ukraine
[b] Department of Chemistry and Geography, Faculty of Natural Sciences and Mathematics, Daugavpils University, 13 Vienibas, Daugavpils LV5401, Latvia
[c] Department of Biomedical Engineering and Computational Science, School of Science and Technology, Aalto University, Espoo FI-00076, Finland

ARTICLE INFO

Article history:
Received 22 January 2012
In final form 22 February 2012
Available online 3 March 2012

ABSTRACT

A series of novel fluorescent aminobenzanthrone dyes have been tested for their ability to identify and characterize the oligomeric and fibrillar aggregates of lysozyme. The parameters of the dye binding to native, oligomeric and fibrillar protein have been calculated from the results of fluorimetric titration. Furthermore, several additional quantities reflecting the preference of the probe to either pre-fibrillar or fibrillar protein aggregates, have been evaluated. Based on the comparative analysis of the recovered parameters, AM4 was recommended for selective detection of protein pre-fibrillar assemblies, while the dyes AM1, AM2, AM3 were selected as the most prospective amyloid tracers.

1. Introduction

A great number of so-called conformational diseases, including neurological disorders (Parkinson's, Alzheimer's and Huntington's diseases), type II diabetes, spongiform encephalopathies, thyroid carcinoma, systemic amyloidosis, etc., are strongly associated with the deposition in tissues of highly ordered pathogenic protein aggregates, called amyloid fibrils. Amyloidogenesis refers to an *in vivo* process in which one of the human amyloidogenic proteins abnormally self-associates into a fibril 60–100 E in width and of a variable length. Amyloid fibrils share a characteristic cross-β-sheet structure with β-strands orienting perpendicular to long axis of the fibril and β-sheets propagating in its direction. The driving forces for amyloid assembly *in vivo* are thought to involve heat shock, oxidative stress or gene mutations, while *in vitro*, the conditions favoring fibril formation include lowering pH, elevating temperature, adding organic solvents or denaturants, etc.

Given the crucial role of protein fibrillar aggregates in the development of debilitating diseases, correct identification and accurate characterization of amyloid assemblies are of utmost importance. The process of fiber formation is being studied with a vast majority of powerful techniques including transmission electron and atomic force microscopy [1,2], nuclear magnetic and electron paramagnetic resonance [3,4], circular dichroism (CD) [2,5], X-ray diffraction analysis [6], fluorescence spectroscopy [7], etc. Of these, the method based on the measurement of Thioflavin T (ThT) fluorescence is one of the gold standards for protein fibril detection [8]. Though being widespread, this assay suffers from several drawbacks: (i) high affinity of ThT for native proteins and bacteria; (ii) slow binding kinetics; (iii) sensitivity to amino acid sequence, pH and ionic strength of solution [9,10]. In view of this, a wide range of novel fluorophores, such as, for instance, T-49 [11], T-284 [12], DCVJ [8], ANS, TNS [13], stilbene derivatives [14], CRANAD-2 [15] have been developed for both *in vivo* and *in vitro* amyloid detection. Ideally, a prospective amyloid marker should fulfill the following requirements: (i) high affinity for protein aggregates ($\sim$1 μM^{-1}), (ii) high quantum yield, extinction coefficient ($\sim 10^4\ M^{-1}\ cm^{-1}$), Stokes shift and binding stoichiometry, (iii) low background fluorescence, (iv) photo- and chemical stability, (v) nontoxicity for living cells [16]. Despite the broad selection of available fluorophores, fibril tracers that fully meet the above challenges have to be found. Our previous work revealed one prospective fluorescent probe, benzanthrone derivative ABM, sensitive to the presence of amyloid aggregates [17]. Cumulative data from the binding, resonance energy transfer and red edge excitation shift (REES) studies allowed us to give comprehensive characteristic of lysozyme (Lz) fibrillar aggregates. Inspired by such unrivalled potential of ABM in identifying the amyloid assemblies, in the present work we evaluated the specificity of a range of novel aminobenzanthrones, referred to here as A4, A6, A8, AM1, AM2, AM3 and AM4, to the protein oligomeric and fibrillar aggregates. More specifically, our goals were: (i) to identify the fluorophores possessing the highest sensitivity to lysozyme pre-fibrillar and fibrillar aggregates; (ii) to quantitatively characterize the dye binding to native, oligomeric and fibrillar lysozyme; and (iii) to analyze the properties of putative binding sites for aminobenzanthrones in amyloid fibrils.

* Corresponding author. Address: 12-38 Aeroflotskaya Str., Kharkov 61031, Ukraine.
E-mail address: katenka_vus@mail.ru (K. Vus).

0009-2614/$ - see front matter © 2012 Elsevier B.V. All rights reserved.
doi:10.1016/j.cplett.2012.02.061

2. Materials and methods

2.1. Chemicals

Chicken egg white lysozyme was purchased from Sigma (St. Louis, MO, USA). Seven fluorescent probes, A4, A6, A8, AM1, AM2, AM3, AM4 (Figure 1), were synthesized at the Faculty of Natural Sciences and Mathematics of Daugavpils University by a nucleophilic substitution of the mobile bromine atom in 3-aminobenzanthrone, as described previously [16].

2.2. Preparation of lysozyme fibrils

Protein solution (3 mg/ml) was prepared by dissolving lysozyme in deionized water with subsequent slow addition of ethanol to a final concentration 80%. Next, the samples were subjected to constant agitation at ambient temperature (over a time course of about 30 days) to obtain lysozyme fibrils [2]. The amyloid nature of fibrillar aggregates was confirmed in ThT assay. Both mature and immature (after 13 days of agitation, containing mostly oligomers) fibril assays were withdrawn from the tube to conduct the fluorescence measurements. Native lysozyme solution (3 mg/ml) in sodium phosphate buffer (pH 7.4) was also used for the fluorimetric titration.

2.3. Steady-state fluorescence measurements

Steady-state fluorescence spectra were recorded with LS-55 spectrofluorimeter equipped with a magnetically stirred, thermostated cuvette holder (Perkin–Elmer Ltd., Beaconsfield, UK). Fluorescence measurements were performed at 20 °C using 10 mm path-length quartz cuvettes. Emission spectra were recorded in buffer and in the presence of native, fibrillar and pre-fibrillar lysozyme with excitation wavelengths of 490 nm for A4, 450 nm for A6, AM2 and AM3, 440 nm for A8 and AM1, 470 nm for AM4. The excitation and emission slit widths were set at 10 nm.

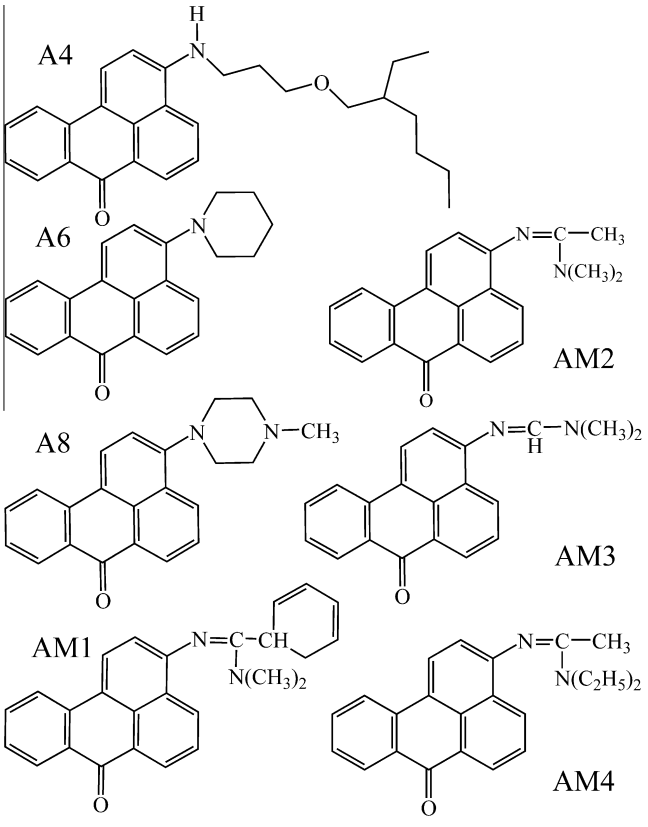

Figure 1. Structural formula of 3-bromobenzanthrone derivatives.

2.4. Binding model

Quantitative characteristics of the dye binding to lysozyme were determined in terms of the Langmuir adsorption model by analyzing the protein-induced changes in probe fluorescence intensity at the wavelengths, corresponding to emission maxima for each dye (570–650 nm, Table 1). It was assumed that the measured fluorescence intensity change (ΔI) is proportional to the concentration of the bound probe (B_Z):

$$\Delta I = I - I_0 = a_{\text{bound}} B_Z + a_{\text{free}}(Z_0 - B_Z) - a_{\text{free}} Z_0 = (a_{\text{bound}} - a_{\text{free}}) B_Z = \alpha B_Z \quad (1)$$

where a_{bound} and a_{free} stand for molar fluorescence of the bound and free dye, respectively, Z_0 is the total concentration of the probe. If one protein molecule contains n dye binding sites, the association constant (K_α) is given by:

$$K_\alpha = \frac{B_Z}{(Z_0 - B_Z)(nC_P - B_Z)} \quad (2)$$

where C_P is the total protein concentration. Eqs. (1) and (2) can be rearranged to give:

$$\Delta I = 0.5\alpha\left[Z_0 + nC_P + 1/K_\alpha - \sqrt{(Z_0 + nC_P + 1/K_\alpha)^2 - 4nC_P Z_0}\right] \quad (3)$$

Approximation of the experimental dependencies $\Delta I(C_P)$ by Eq. (3) allowed us to determine the dye–protein binding parameters (K_α, n and α).

2.5. Quantum yield calculation

Quantum yields of the dyes in free and protein-bound states were calculated as [18]:

$$Q = \frac{Q_S(1 - 10^{-A_S})S_D}{(1 - 10^{-A_D})S_S} \quad (4)$$

where Q_S is the quantum yield of a standard dye (Rhodamine 101) (~1), S_D and S_S are the integrated areas of the fluorescence spectra of dye and standard, respectively, A_D and A_S are the absorbances of the dye and standard at excitation wavelength, respectively. Absorption measurements were performed with SF-46 spectrophotometer in 2 mm quartz cuvette.

3. Results and discussion

Irrespective to protein conformation (native, oligomeric or fibrillar), the complexation of aminobenzanthrones with lysozyme was accompanied by significant increase in the probe fluorescence intensity and blue shift of emission maximum for some dyes (Tables 1–3). These effects can be explained by fluorophore transfer into the less polar and motionally restricted membrane environment. In this respect, it is noteworthy that amyloid sensitive probe Nile Red also showed blue shift of its emission maximum upon association with lysozyme fibrils, as reported by Mishra and coworkers [19]. However, this property is not general for amyloid specific dyes, since, for instance, Michler's hydrol blue, another fluorophore used for detection of lysozyme amyloid plaques, displays red shift of its emission maximum in the presence of amyloid fibrils [20].

Table 1
Quantitative characteristics of aminobenzanthrone binding to native lysozyme.

Dye	A4	A6	A8	AM1	AM2	AM3	AM4	ThT
Excitation, nm	490	450	440	450	450	450	470	412
Emission maximum, nm	636	596	584	619	596	593	567	480
K_α, μM^{-1}	0.9 ± 0.2	–	–	–	5.4 ± 1.2	0.9 ± 0.2	0.2 ± 0.04	0.03 ± 0.01
n, mol/mol	2 ± 0.4	–	–	–	1.9 ± 0.4	2.2 ± 0.4	1.6 ± 0.5	10.3 ± 3.4
α, μM^{-1}	0.5 ± 0.1	–	–	–	1.9 ± 0.5	7.5 ± 1	8 ± 2	7.1 ± 1.8
Blue shift of emission maximum, nm	0	0	7	2	0	2	0	0
I^*_{nat}/I^*_0	1.2	–	–	–	1.1	1.3	1.1	1.3
Q_B	0.06	–	–	–	0.07	0.11	0.09	0.009

Table 2
Quantitative characteristics of aminobenzanthrone binding to oligomeric lysozyme.

Dye	A4	A6	A8	AM1	AM2	AM3	AM4
K_α, μM^{-1}	0.8 ± 0.2	5.7 ± 0.02	13.7 ± 4.5	14.2 ± 4.1	1 ± 0.2	21.6 ± 6.5	0.3 ± 0.01
n, mol/mol	0.14 ± 0.05	0.19 ± 0.05	0.14 ± 0.03	0.07 ± 0.02	0.23 ± 0.06	0.11 ± 0.03	0.98 ± 0.2
α, μM^{-1}	20 ± 4	159 ± 42	71 ± 15	454 ± 35	90 ± 25	235 ± 75	200 ± 70
Blue shift of emission maximum, nm	12	10	36	12	0	7	0
I^*_{olig}/I^*_0	2.6	1.5	1.5	1.5	1.7	2.3	4.9
I^*_{olig}/I^*_{nat}	4.1	–	–	–	2.2	3.6	3.5
Q_B	0.08	0.42	0.3	0.25	0.1	0.48	0.47

Table 3
Quantitative characteristics of aminobenzanthrone binding to fibrillar lysozyme.

Dye	A4	A6	A8	AM1	AM2	AM3	AM4	ThT
K_α, μM^{-1}	2.9 ± 0.7	27 ± 6	1.7 ± 0.15	2 ± 0.5	5 ± 0.2	70 ± 8	2.6 ± 0.2	0.04 ± 0.01
n, mol/mol	0.2 ± 0.04	0.23 ± 0.05	0.22 ± 0.4	0.22 ± 0.03	0.35 ± 0.05	0.56 ± 0.25	0.2 ± 0.06	7.6 ± 2.1
α, μM^{-1}	22 ± 7	118 ± 25	64 ± 15	850 ± 100	190 ± 26	165 ± 35	202 ± 55	22 ± 5
Blue shift of emission maximum, nm	0	14	35	19	0	6	0	0
I^*_{fibr}/I^*_0	5.2	2.4	1.9	5.7	38.4	9.7	3.7	2.8
I^*_{fibr}/I^*_{nat}	3.7	–	–	–	5.0	7.2	3.1	1.2
Q_B	0.06	0.39	0.47	0.66	0.69	0.34	0.5	0.03
REES, nm	7	6	14	21	3.5	2	19.5	–

Typical fluorescence spectra of aminobenzanthrones recorded upon the dye titration with lysozyme are presented in Figure 2A. Notably, in the case of A6, A8 and AM1, elevating concentrations of native lysozyme didn't result in any change of the dye emission. Such a behavior may be a consequence of very low (if any) affinity of these dyes for protein monomers.

Quantitative analysis of the dependencies between the measured fluorescence intensity increase (ΔI) and protein concentration (C_P), presented for illustration in Figure 2B, in terms of the Langmuir adsorption model allowed us to estimate the parameters of aminobenzanthrone complexation with native, oligomeric and fibrillar lysozyme – association constant (K_α), binding stoichiometry (n) and the difference between molar fluorescence of the bound and free dye (α) Likewise, for more accurate comparison of the dye specificity for a certain protein conformation, the following additional quantities have been calculated using the recovered binding parameters (Tables 1–3):

$I^*_{nat,olig,fibr}/I^*_0$ – relative fluorescence intensity increase upon the dye binding to native, oligomeric or fibrillar protein, the asterisk refers to the protein and dye concentrations 2 and 1 μM, respectively;

$I^*_{olig,fibr}/I^*_{nat}$ – specificity of the dyes to protein oligomers or fibrillar aggregates, respectively; Q_B – quantum yield of the protein-bound dye.

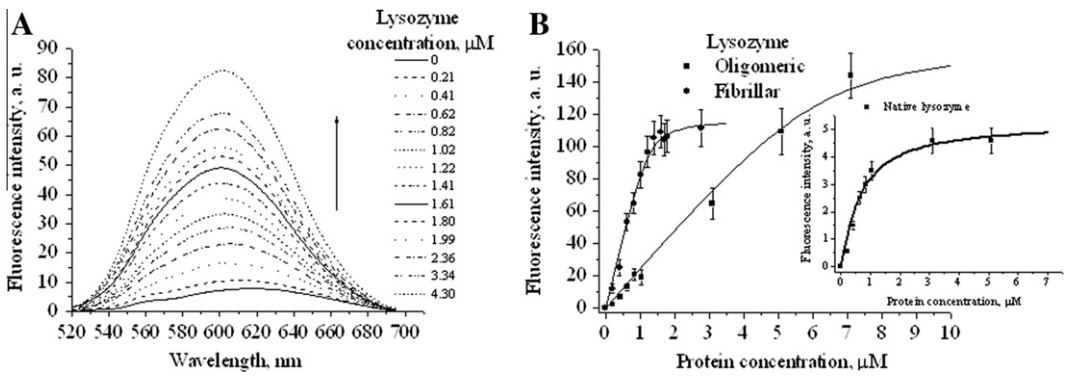

Figure 2. Emission spectra of AM1 recorded upon fluorimetric titration of the dye with fibrillar lysozyme. AM1 concentration was 0.1 μM (A). The isotherms of AM3 binding to oligomeric, fibrillar and native (inset) lysozyme. Dye concentration was 0.7 μM (B).

In order to compare the properties of the novel dyes with those of the classical amyloid marker, all the above parameters have been derived also for ThT. This allowed us to range the aminobenzanthrones according to their specificity to oligomeric or fibrillar protein (Table 4). It appeared that in the presence of lysozyme pre-fibrillar aggregates AM4 showed the highest fluorescence intensity increase on going from the aqueous phase to protein matrix, while the binding preferences were the best for A6, A8, AM1 showing no affinity for native lysozyme. Interestingly, AM4 has similar K_α for native and oligomeric protein, but higher association constant for fibrillar protein. However, the contribution of other parameters, such as n and α into I^*_{olig}/I^*_0 and I^*_{olig}/I^*_{nat} seems to dominate over K_α contribution, resulting in the higher specificity of this aminobenzanthrone to lysozyme oligomers compared to fibrillar structures (Table 4). Our findings strongly suggest that AM4 can be used for selective detection of protein pre-fibrillar assemblies which are thought to be the most toxic species [21].

In the case of mature fibrils, the highest binding preference was found for AM2 dye (Table 4). This probe showed the most pronounced relative intensity increase (*ca.* 38) and the greatest quantum yield in protein-bound state (*ca.* 0.7). For the sake of comparison, analogous parameters for ThT attain the values of 2.8 and 0.03, respectively. Furthermore, I^*_{fibr}/I^*_{nat} ratio for AM2 exceeds that observed for ThT by a factor of ~4. AM1 takes second place in the total row, indicating a decrease in the dye specificity to fibrillar protein. Intriguingly, these two dyes can distinguish between mature fibrils and protein oligomers, showing the lower specificity to oligomeric lysozyme (Tables 2 and 3). Moreover, AM1 possesses an additional advantage, such as virtually no binding to monomeric protein. Another dye that showed good preference for lysozyme fibrils is AM3. The association constant for complexation of this dye with fibrillar lysozyme ($K_\alpha = 70\ \mu M^{-1}$) is about two orders of magnitude higher than that for native protein ($K_\alpha = 0.9\ \mu M^{-1}$). Likewise, AM3 is featured by rather high value of I^*_{fibr}/I^*_0 (*ca.* 10). Given all these rationales, the above three dyes, viz., AM1, AM2 and AM3 can be recommended as novel amyloid tracers, representing a good alternative for ThT. It should be noted in this context that aminobenzanthrones are similar in their spectral properties to amyloid specific probe Nile Red [19].

In principle, as seen from our results, all aminobenzanthrones can be employed for spectral differentiation between monomeric and self-associated protein. For example, spectral parameters of A6, A8 and AM1 did not undergo any marked changes upon the dye binding to native lysozyme, while complexation of these fluorophores with pre-fibrillar or fibrillar aggregates was accompanied by the increase in fluorescence intensity and blue shift of the emission maximum. Hence, it can be assumed that these dyes bind only to the protein aggregates, but not to the monomers. This permits the tracing of self-assembled protein species, although the identification of exact conformation of these species (oligomeric or fibrillar) may be hampered. Taken together, all dyes under study showed much stronger affinity for lysozyme fibrils than ThT, as judged from the comparison of I^*_{fibr}/I^*_0, I^*_{fibr}/I^*_{nat}, Q_B and K_α values.

At the next step of the study we focused our efforts on analyzing the effect of solvent dynamics on the spectral properties of aminobenzanthrone dyes by examining the red edge excitation shifts (REES) (Figure 3). REES manifests itself as a red shift in fluorescence spectra caused by the shift in excitation wavelength toward the red edge of absorption band. REES arises from the slowed rates of solvent relaxation around the excited fluorophore which reflects the motional restrictions imposed on the solvent molecule in the immediate vicinity of the dye [22,23]. Although REES phenomenon is used mainly for monitoring of water mobility in biological membranes, it can be also successfully employed in exploring the solvent reorientation dynamics in mature amyloid fibrils, especially the dynamics of water which may penetrate into amyloid hydrophobic cavities, thereby optimizing intermolecular sheet-sheet packing [24,25]. As shown in Table 3, all aminobenzanthrones exhibited REES. According to the REES values, the dyes under study can be tentatively divided into three groups: (i) AM2 and AM3, displaying low REES (3.5 and 2 nm, respectively), (ii) A4 and A6, characterized by moderate REES (7 and 6 nm, respectively), and (iii) A8, AM1 and AM4, with high magnitude of REES (14, 21 and 19.5 nm, respectively). As was proposed by Chattopadhyay et al., REES values may be used to determine the depth of the probe penetration into biological matrices (so-called 'dipstick' rule) [26]. Specifically, it was shown that REES magnitude varies in direct correlation with the depth of probe penetration in the lipid bilayer – the less the REES, the deeper is the probe membrane location. Accordingly, high REES is generally attributed to the interfacial and polar regions of membranes, while low or no REES is typical for hydrophobic part of the lipid bilayer. Assuming the same mechanism for amyloid structures, we can make some assumptions about the location of aminobenzanthrones in lysozyme fibrillar aggregates (Figure 4). In terms of the modern models of amyloid structure it is supposed that fibril β-strands form two distinct sheet interfaces, termed dry and wet interfaces [27,28]. The former involves interdigitation of complementary side chains via van der Waals interactions and H-bonds, while the latter is stabilized mainly by H-bonds between the side chains and water molecules in a fashion similar to forming intermolecular contacts in protein crystals [29]. In fact, non-hydrated cavities located deeply in the fibril interior may form the dry interface. In turn, wet interface is completely hydrated and

Table 4

Dye rows showing decrease of aminobenzanthrone specificity to oligomeric protein							
I^*_{olig}/I^*_0	AM4	A4, AM3*	AM2, A6, A8, AM1				
I^*_{olig}/I^*_{nat}	A6, A8, AM1 showed no affinity for native lysozyme		A4, AM3, AM4			AM2	
Q_B	AM3, AM4	A6	A8	AM1	AM2	A4	
Total row	AM4	AM3	A6	A8	AM1	A4	AM2
Dye rows showing decrease of aminobenzanthrone specificity to fibrillar protein							
I^*_{olig}/I^*_0	AM2	AM3	AM1	A4	AM4	ThT	A6, A8
I^*_{olig}/I^*_{nat}	A6, A8, AM1 showed no affinity for native lysozyme		AM3	AM2	A4	AM4	ThT
Q_B	AM2, AM1	AM4, A8	A6, AM3	A4, ThT			
Total row	AM2	AM1	AM3	A6	AM4	A8	A4	ThT

* The list of the dyes, divided by comma, indicates that they display close values of the parameters $I^*_{olig.fibr}/I^*_0$, $I^*_{olig.fibr}/I^*_0$ or Q_B.

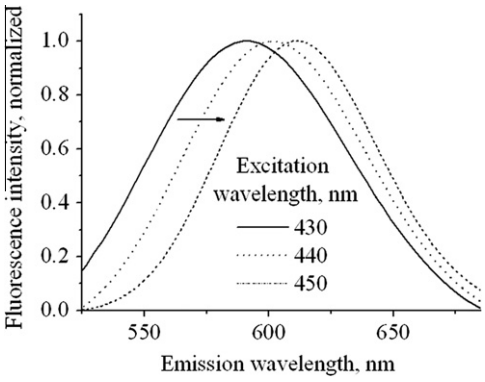

Figure 3. Red edge excitation shift of AM1 bound to fibrillar lysozyme. Dye and protein concentrations were 0.1 and 4.3 μM, respectively (A,B).

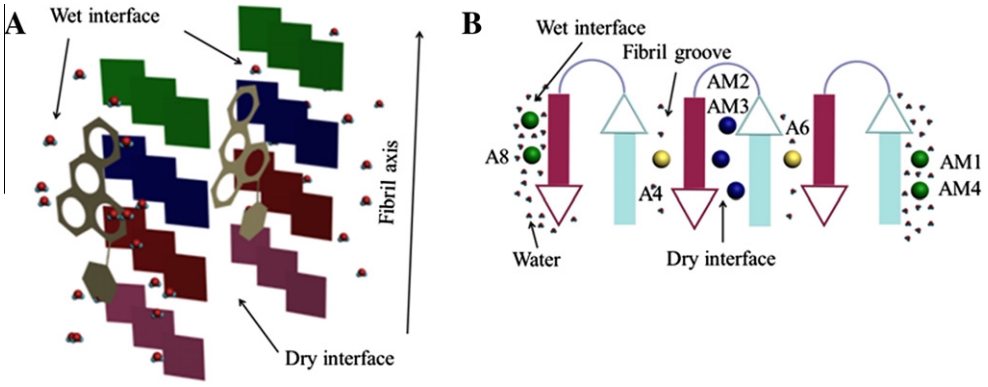

Figure 4. Side (A) and top (B) views on lysozyme amyloid fibril. Top view shows only wet and dry interfaces. A8, AM1, AM4 are supposed to associate with the wet interface, while AM2 and AM3 prefer the dry interface (A). The environment of intermediate hydrophobicity where A4 and A6 are presumably located is represented by fibril grooves (B).

virtually represents the fibril surface. By analogy with 'dipstick' rule, formulated for the lipid bilayers, it may be anticipated that A8, AM1 and AM4, displaying high REES values, reside at the wet interface of lysozyme fibrils, i.e. bind to the surface of fibrillar aggregate, while AM2 and AM3, whose REES is very low, locate at the dry interface, embracing deep cavities in the fibril interior. The presence of small amount of water in such cavities was demonstrated in a number of studies for different proteins and was shown to play the critical role in stabilizing the amyloid structure [30,31]. The moderate REES magnitude observed for A4 and A6, is suggestive of fluorophore location somewhere between the wet and dry interfaces. Obviously, these dyes are buried in the amyloid grooves created by the aligned side chains in the fibril axis, where hydration level is higher than that at the dry interface, but at the same time lower than at the wet interface.

Based on the REES analysis some possible correlations between the relative intensity increases I^*_{fibr}/I^*_0 and binding locations of the dyes can be suggested. The dyes AM2 and AM3, probably located at the fibril dry interface according to their REES values, display the highest I^*_{fibr}/I^*_0 (*ca.* 38 and 10, respectively), that is in agreement with the general property of aminobenzanthrones to respond to decrease of the environmental polarity by quantum yield increase [16,32]. Analogous quantum yield behavior is characteristic of the aminobenzanthrone ABM (structurally very close to the dyes under investigation) used in cell membranes studies as lipophilic probe [33,34]. The difference in I^*_{fibr}/I^*_0 of AM2 and AM3 dyes can be explained by their different sensitivity to the polarity changes. It is known that the substituent at the C-3 position of the benzanthrone molecule determines the power of the donor (3-aminosubstituent) – acceptor (carbonyl group of the benzanthrone molecule) interaction after the excitation. The dyes having the 3-aminosubstituent with lower electron-donating power display lower sensitivity to the environmental polarity, viscosity, etc. [35,36]. The above observations lead us to the conclusion that despite similar location of AM2 and AM3, the lower I^*_{fibr}/I^*_0 and REES values of AM3, reflect its weaker donor–acceptor interactions, or lower polarity sensitivity.

With regard to the dyes, probably bound to more polar fibril sites, i.e. fibril surface or amyloid grooves, the high REES values indicate their inability to penetrate deeper into fibril core and reach hydrophobic cavities (obviously because of the bulkier 3-aminosubstituents of these dyes compared to AM2 and AM3). This leads to the lower I^*_{fibr}/I^*_0 values of the lipophilic aminobenzanthrones compared to those of AM2 and AM3. On the other hand, the I^*_{fibr}/I^*_0 ratios of the dyes occupying fibril grooves and surface sites are similar. So, it can be supposed that two different lysozyme fibril binding sites differ insignificantly in their polarity due to water penetration into the fibril grooves. At the same time, the higher REES of A4 and A6 presumably bound to the grooves than that of surface-bound A8, AM1, AM4 can be explained by lower water mobility in the grooves of lysozyme fibrils compared to their surface [22,26].

By and large, the majority of aminobenzanthrone dyes possess the fibril specificity (Table 4, total row), decreasing with the increase of protein binding site polarity assessed from REES analysis.

In conclusion, the present study has been undertaken to evaluate the potential of the novel aminobenzanthrone dyes to selectively detect pre-fibrillar and fibrillar protein aggregates. All dyes displayed very high efficiency of binding to the aggregated lysozyme. Furthermore, novel probes showed much higher affinity for the amyloid fibrils than classical amyloid marker Thioflavin T. Based on comprehensive analysis of the spectral characteristics of aminobenzanthrones bound to native, oligomeric and fibrillar lysozyme, we recommend the dye AM4 for selective detection of protein pre-fibrillar assemblies, while the dyes AM1, AM2 and AM3 can be employed as novel amyloid tracers.

Acknowledgments

GG gratefully acknowledges a visiting scientist award by the Sigrid Juselius Foundation. This work was supported by the grants from European Social Fund (project number 2009/0205/1DP/1.1.1.2.0/09/APIA/VIAA/152), the Science and Technology Center in Ukraine (project number 4534), Fundamental Research State Fund (project number F.41.4/014) and young scientist award by the President of Ukraine to VT (project number GP/F32/109).

References

[1] P. Shahi, R. Sharma, S. Sanger, I. Kumar, R.S. Jolly, Biochemistry 46 (2007) 7365.
[2] M. Holley, C. Eginton, D. Schaefer, L.R. Brown, Biochem. Biophys. Res. Commun. 373 (2008) 164.
[3] R. Tycko, Curr. Opin. Struct. Biol. 1 (2004) 96.
[4] M. Margittai, R. Langen, Q. Rev. Biophys. 41 (2008) 265.
[5] G. Merlini, V. Bellotti, N. Engl. J. Med. 349 (2003) 583.
[6] M. Sunde, C.C. Blake, Q. Rev. Biophys. 31 (1998) 1.
[7] B.W. Koo, A.D. Miranker, Protein Sci. 14 (2005) 231.
[8] M. Lindgren, K. Sırgjerd, P. Hammarstrıım, Biophys. J. 88 (2005) 4200.
[9] M. Groenning, J. Chem. Biol. 3 (2010) 1.
[10] M. Biancalana, K. Makabe, A. Koide, S. Koide, J. Mol. Biol. 385 (2009) 1052.
[11] K.D. Volkova, V.B. Kovalska, A.O. Balanda, R.J. Vermeij, V. Subramaniam, Y.L. Slominskii, S.M. Yarmoluk, J. Biochem. Biophys. Methods 70 (2007) 727.
[12] K.D. Volkova et al., J. Fluoresc. 20 (2010) 1267.
[13] M.S. Celej, E.A. Jares-Erijman, T.M. Jovin, Biophys. J. 94 (2008) 4867.
[14] M.S. Hong et al., Bioorg. Med. Chem. 18 (2010) 7724.
[15] C. Ran, X. Xu, S.B. Raymond, Am. Chem. Soc. 131 (2009) 15257.
[16] E.M. Kirilova, I. Kalnina, G.K. Kirilov, I. Meirovics, J. Fluoresc. 18 (2008) 645.
[17] G. Gorbenko et al., Chem. Phys. Lett. 495 (2010) 275.
[18] B. Valeur, Molecular Fluorescence: Principles and Applications, Wiley-VCH, New York, 2001.

[19] R. Mishra, D. Sjıılander, P. Hammarstrıım, Mol. Biosyst. 7 (2011) 1232.
[20] C.C. Kitts, T. Beke-Somfai, B. Nordén, Biochemistry 50 (2011) 3451.
[21] C.G. Glabe, Neurobiol. Aging 27 (2006) 570.
[22] J.R. Lakowicz, Principles of Fluorescent Spectroscopy, third adn., Springer, New York, 2006.
[23] A. Chattopadhyay, Chem. Phys. Lipids 122 (2003) 3.
[24] J. Zheng, H. Jang, B. Ma, C.J. Tsai, R. Nussinov, Biophys. J. 93 (2010) 3046.
[25] Y.S. Kim, L. Liu, P.H. Axelsen, R.M. Hochstrasser, PNAS 106 (2009) 17751.
[26] A. Chattopadhyay, S. Mukherjee, Langmuir 15 (1999) 2142.
[27] M.R. Sawaya et al., Nature 447 (2007) 453.
[28] M.I. Ivanova, S.A. Sievers, M.R. Sawaya, J.S. Wall, D. Eisenberg, PNAS 106 (2009) 18990.
[29] R. Nelson, M.R. Sawaya, M. Balbirnie, A.O. Madsen, C. Riekel, R. Grothe, D. Eisenberg, Nature 435 (2005) 773.
[30] Y.H. Lee, E. Chatani, K. Sasahara, H. Naiki, Y. Goto, J. Chem. Biol. 284 (2009) 2169.
[31] T. Yamazaki, N. Blinov, D. Wishart, A. Kovalenko, Biophys. J. 95 (2008) 4540.
[32] E. Kirilova, I. Ivanova, Sci. J. Riga Tech. Univ. 23 (2011) 29.
[33] T.S. Dyubko et al., Tsitologiya 49 (2007) 521.
[34] I. Kalnina, E. Kirilova, L. Klimkane, J. Immunotoxicol. 6 (2009) 293.
[35] M. Nepras, O. Machalicky, M. Seps, R. Hrdina, P. Kapusta, V. Filder, Dyes Pigm. 35 (1997) 31.
[36] I. Grabchev, V. Bojinov, I. Moneva, Dyes Pigm. 48 (2001) 143.